International Journal of Current Bio-Medical Engineering (IJCBE)
Volume 4, Issue 1, January – February (2026)

RESEARCH ARTICLE

AUD PFS: ATTENTION U-NET BASED DEEP LEARNING FRAMEWORK FOR ACCURATE PULMONARY FIBROSIS SEGMENTATION IN MEDICAL IMAGES

Godlin Atlas L[1,*] and Vaishnavi V[2]

[1]Associate professor, Department of Computer Science and Engineering, Bharath Institute of Science and Technology (BIST), 173, Agaram road, Selaiyur, Tambaram, Chennai, Tamilnadu, 600073, India.
[2]Assistant Professor, Department of Electrical and Electronics Engineering, Sethu Institute of Technology, Kariapatti, Tamilnadu, 626115, India.

[*]*Corresponding e-mail: godlinatlas.cse@bharathuniv.ac.in*

Abstract – Pulmonary fibrosis (PF) is a chronic lung disorder in which the lung tissue becomes permanently scarred of early detection and accurate segmentation plays an important role in proper diagnosis and planning of the best treatment. However most existing approaches often provide only quantitative predictions without generating detailed binary, color-coded, and overlay segmentation outputs that can assist clinicians in visualizing fibrosis-affected regions. To address this issue, a novel Deep Learning (DL)-based AUD PFS model for PF segmentation is suggested, which uses CT images from the OSIC Pulmonary Fibrosis Progression Dataset. The hybrid Median with Weiner (MedWe) filter is used to improve the CT image and to remove the noise in the images. ResNet50 is used to extract the feature from the CT image for reliable segmentation and Attention UNet is employed for segmenting the CT images of PF as Binary segmentation, color-codded segmentation and Overlay segmentation. The proposed AUD PFS is evaluated using the following metrics: accuracy, precision, recall, specificity, F1-score, Dice index, and Jaccard index. From the experimental analysis, the proposed AUD PFS model attains an overall accuracy of 99.02% and F1-score of 97.23% for efficient PF segmentation. Moreover, the proposed AUD PFS model improves the overall accuracy by 1.53%, 0.02%, 13.85%, 9.11% and 5.17% better than ResNet18-based U-Net, nnU-Net, HCR-DL model, CNN, and AE-IPF respectively.

Keywords *– Pulmonary fibrosis, Deep Learning, resNet50, Attention UNet, Binary segmentation.*

1. INTRODUCTION

This Lung cancer is the leading cause of cancer-related fatalities globally, with 2.09 million new cases and 1.76 million deaths in 2018. Pulmonary Fibrosis (PF), caused by inflammation and scarring of lung tissues, is a typical radiation-induced damage in lung cancer treatment. This can cause breathing difficulties, lung damage, and, in severe cases, lung failure [1]. Idiopathic Pulmonary Fibrosis (IPF) is caused by increasing scarring (fibrosis) of the lung tissue due to aberrant wound-healing processes, but the exact reason is unknown [2, 3]. IPF causes gradual shortness of breath, a dry cough, and decreased lung function as lung fibrosis progresses [4]. Dyspnea (difficulty breathing) and hypoxia (low oxygen levels in the blood) are the primary symptoms of pulmonary fibrosis when lung scarring worsens [5].

Idiopathic pulmonary fibrosis (IPF) is a severe lung ailment with a median survival duration of two to five years an incidence of 0.9-13 cases per 100,000 people, and a frequency of 3.3-29.8 cases per 100,000. Idiopathic pulmonary fibrosis [6, 7]. The study investigated 21 IPF patients and 59 healthy controls and found that pulmonary vascular capacity was considerably greater in IPF patients (60.9 mL vs 22.0 mL; $p < 0.001$) [8]. High-Resolution Computed Tomography (HRCT) was combined with an AI-based deep learning semantic segmentation system to analyze CT lung images and detect fibrotic (honeycomb) regions for disease assessment and death prediction [9]. Volumetric HRCT chest scans were integrated with the AirQuant automated airway analysis tool to quantify airway shape in idiopathic pulmonary fibrosis (IPF). AirQuant assessed airway properties such as intersegmental tapering and tortuosity from CT scans [10].

The development of Artificial Intelligence (AI) has produced promising result in PF segmentation [11]. Deep Learning (DL) algorithms like CNN [12] and ResNet are widely used for disease segmentation [13]. Machine Learning (ML) algorithms like SVM, Kernel Fuzzy C-Mean demonstrated remarkable performance for segmentation [14, 15]. However, most existing studies focus on IPF diagnosis,

classification, prognosis prediction, and mortality assessment rather than the precise segmentation of pulmonary fibrosis regions. To overcome this issue a novel AUD PFS model is proposed for accurate segmentation of PF. The key contribution of PF is listed below,

- The MedWe filter is the combination of Median and Weiner filter to remove the noise and enhance the CT images from OSIC Pulmonary Fibrosis Progression Dataset.
- The ResNet50 is used to extract the feature of PF from the CT image for reliable segmentation of PF.
- The proposed AUD PFS model uses Attention UNet to segment the PN from ResNet50 as Binary segmentation, color-coded segmentation and overlay segmentation.
- The proposed AUD PFS model performance was assessed using Accuracy, Precision, Recall, Specificity, F1-score, Dice Index and Jaccard Index for efficient PF segmentation.

The remainder of the research was structured as follows. The literature review is defined in Section 2. Section 3 describes the proposed AUD PFS model for segmenting PF based on CT images. Section 4 analyzes and validates the proposed AUD PFS model's results using various metrics. Section 5 provides the conclusion and future work.

2. LITERATURE SURVEY

Several research have been conducted to segment PF using a range of ML and DL methodologies. Researchers investigate various model architectures, feature extraction approaches and optimization techniques for improving classification performance. These provides a comparative review of existing methodologies that includes suggested techniques and achieved accuracies.

In 2025 Kaur, et al., [16] suggested various machine learning classifiers to identify the best classifier for both original and pre-processed images. Machine Learning classifiers such as including Naive Bayes (NB), K Nearest Neighbors (KNN), Decision Tree (DT), Logistic Regression (LR), and Support Vector Machine (SVM). The SIFT + HOG + LBP feature extraction, combined with Logistic Regression achieves an accuracy of 97.12%.

In 2024, Sanida, T., et al., [17] introduced an optimized Deep Learning model to perform multi-label classification of CXR images with a customized VGG16 architecture with Squeeze-and-Excitation (SE) blocks. The updated VGG16-SE model outperformed all tested measures. The model had an accuracy of 98.49%.

In 2024, Dikmen, O., [18] suggested various deep learning models, including VGG19, ResNet18, and a ResNet18-based U-Net, as well as a custom Convolutional Neural Network (CNN) developed in MATLAB, for the classification and segmentation of lung X-ray images. The VGG19 model utilizing transfer learning, demonstrated strong diagnostic capabilities, achieving high accuracy rates for COVID-19, lung opacity, healthy lungs, and viral pneumonia classification, with a test accuracy of 97.5%.

In 2024 Thillai et al., [19] developed a deep learning-based CT image segmentation algorithm that can autonomously separate lung, vascular, fibrosis, and airway regions in IPF patients. The approach was utilized to develop imaging biomarkers for disease progression and death prediction. The model had a 97.8% segmentation success rate and had a good connection with lung function ($r = 0.82$), indicating its usefulness in IPF assessment.

In 2024 Dwivedi et al., [20] created a nnU-Net-based lung segmentation model to automatically separate lungs from CT pulmonary angiography (CTPA) images in patients with pulmonary hypertension and interstitial lung disease. The approach was used to estimate lung capacity and quantify parenchymal disease. The model has a mean accuracy of 99.8%, a Dice Similarity Coefficient (DSC) of 99.0%, and a Normalized Surface Distance (NSD) of 98.3%, indicating very accurate and robust lung segmentation.

In 2022 Refaee, T., et al., [21] created Handcrafted Radiomics (HCR), Deep Learning (DL), and an ensemble HCR-DL model to classify IPF and non-IPF Interstitial Lung Diseases (ILDs) using HRCT images. The ensemble technique improved diagnostic performance by combining radiomics and deep learning characteristics. The suggested ensemble model obtained 85.3% accuracy and an AUC of 0.917, beating both individual models and clinical experts.

In 2023 Maddali, M.V., [22] created a deep learning Convolutional Neural Network (CNN) that uses CT images to automatically differentiate Idiopathic Pulmonary Fibrosis (IPF) from other Interstitial Lung Diseases (ILDs). The procedure was utilized to aid in non-invasive diagnosis and minimize the necessity for surgical lung biopsy. The proposed model's AUC was 0.87, with a sensitivity of 67% and a specificity of 90%, indicating consistent performance in IPF classification.

In 2024 Huang, X., [23] devised a 3D deep learning method (SlowFast network) that uses high-resolution CT (HRCT) images to classify Acute Exacerbation of Idiopathic Pulmonary Fibrosis (AE-IPF). The approach was utilized to detect AE-IPF automatically, assisting radiologists with diagnosis and disease progression evaluation. The model attained an accuracy of 93.9% and 86.5% on two independent test sets, respectively, with ROC-AUC values of 0.96 and 0.92, indicating excellent diagnostic performance.

From the literature survey, most existing studies focus on IPF diagnosis, classification, prognosis prediction, and mortality assessment rather than the precise segmentation of pulmonary fibrosis regions and existing approaches often provide only quantitative predictions without generating detailed binary, color-coded, and overlay segmentation outputs that can assist clinicians in visualizing fibrosis-affected regions. To overcome this issue a novel AUD PFS model is proposed for reliable segmentation.

3. PROPOSED AUD PFS METHODOLOGY

In this section, a novel AUD PFS model is introduced to segment Pulmonary Fibrosis from CT images. The Schematic representation of the proposed AUD PFS model is illustrated in figure1.

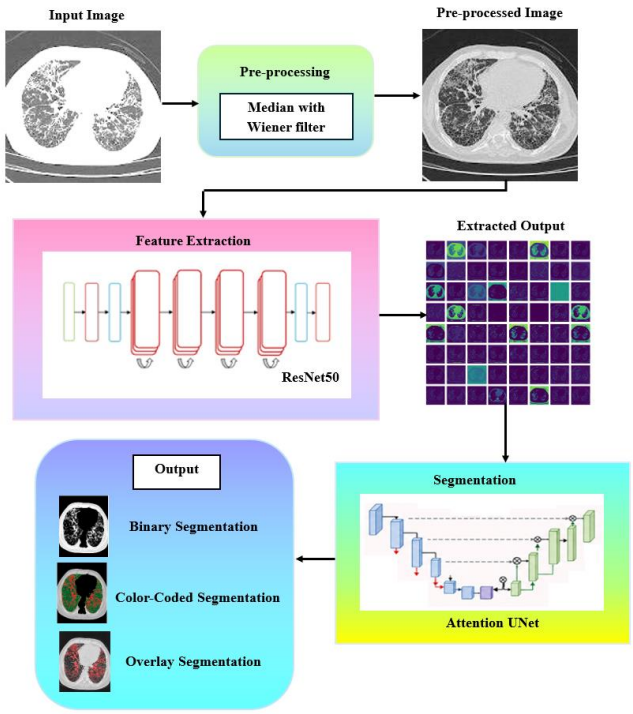

Figure 1: Schematic Representation of the proposed AUD PFS model

3.1 Dataset Description

The proposed AUD PFS method makes use of the OSIC Pulmonary Fibrosis Progression Dataset, which contains roughly 24,647 HRCT lung images obtained from 176 patients with pulmonary fibrosis. The dataset contains 17,449 fibrosis-affected CT scans and 7,198 normal lung slices in DICOM format with a size of 512 × 512 pixels. To improve model performance and reduce overfitting, data augmentation techniques such as rotation, flipping, zooming, scaling, and brightness adjustment are utilized to increase image diversity and strengthen the pulmonary fibrosis segmentation model.

3.2 MedWe Filter

The Hybrid Median with Wiener (MedWe) Filter is an excellent preprocessing technique for improving CT lung images that combines the noise-removal capabilities of the Median Filter and the Wiener Filter. Compared to the Median Filter, the Wiener Filter is used to remove Gaussian noise and image blur by minimizing the mean square error, but the Median Filter is used to remove impulsive noise while maintaining important edges and structures. These filters provide benefits for image quality, fibrosis boundary definition, and feature extraction and segmentation. The Median Filter operation can be written as:

$$I_R(a,b) = median\{I(u,v),(u,v) \in W \quad (1)$$

where $I_R(a,b)$represents the median-filtered image and W denotes the local neighborhood window. The Wiener Filter is defined as:

$$I_W(a,b) = \mu + \frac{\sigma^2 - i^2}{\sigma^2}[I_R(a,b) - \mu] \quad (2)$$

where μ is the local mean, σ^2 is the local variance, and i^2 is the noise variance. The overall Hybrid MedWe filtering method is represented as follows:

$$I_{MedWe}(a,b) = W(R(I(a,b))) \quad (3)$$

where $R(\cdot)$ denotes the Median Filter operation, $W(\cdot)$ denotes the Wiener Filter operation, and $I_{MedWe}(a,b)$ is the final enhanced image used for pulmonary fibrosis feature extraction.

3.3 ResNet50

ResNet50 is a deep CNN that is frequently used for feature extraction in medical picture analysis. It has 50 layers and uses residual learning via skip connections to solve the vanishing gradient problem to extract deep and discriminative features. ResNet50 automatically learns essential texture, edge, and structural properties from CT lung images, resulting in rich feature representations for effective segmentation of pulmonary fibrosis. The residual learning function of ResNet50 is defined as follows:

$$G(a) = F(a) + a \quad (4)$$

where a is the input feature map, $F(a)$ represents the residual mapping learned by the convolutional layers, and $G(a)$ is the output feature map. The convolution operation used for feature extraction is expressed as follows:

$$B(u,v) = \sum_r \sum_s A(u-r, v-s)K(r,s) \quad (5)$$

where A is the input image, K is the convolution kernel, and B is the extracted feature map. ResNet50's activation function is the Rectified Linear Unit (ReLU):

$$f(a) = \max(0, a) \quad (6)$$

ResNet50 is a deep network that extracts hierarchical features from computed tomography (CT) scans, both low-level (such as edges and textures) and high-level (fibrosis patterns). These acquired attributes are then passed to the segmentation network which can accurately locate the site of pulmonary fibrosis.

3.4 Attention UNet

Attention U-Net is used to extract pulmonary fibrosis regions from CT lung images by automatically recognizing aberrant fibrotic tissues and distinguishing them from healthy lung structures. The network is built on an encoder-decoder architecture with attention gates that prioritize clinically significant fibrosis regions over irrelevant background information. The encoder is used for extracting deep features from the CT image, and the attention mechanism is employed to enhance the features related to fibrosis before passing them to the decoder for more accurate segmentation of the CT image. The attention coefficient is calculated as:

$$\alpha = \sigma(W^T(\psi^T(W_a a + W_h h + y_h)) + y_\psi) \quad (7)$$

where α is the attention coefficient, a is the input feature map, h is the gating signal, and σ is the sigmoid activation function. The segmentation accuracy is measured using the DSC:

$$DSC = \frac{2|X \cap Y|}{|X|+|Y|} \quad (8)$$

where X is the predicted fibrosis region and Y is the ground-truth segmentation.

The model creates a binary segmentation image where white is fibrosis and black the background, enabling to clearly identify diseased tissues. The binary mask is then transformed into a color-coded segmentation image, with various colors indicating different areas of fibrosis for easier viewing and interpretation. Last, segmented fibrosis mask is overlaid on the original CT scan and a fibrosis overlay segmented image is created, highlighting the areas of fibrosis without loss of lung anatomy. The three outputs facilitate quantitative analysis, better visualization of pulmonary fibrosis regions and clinical interpretation.

4. RESULT AND DISCUSSION

The result section examines the performances of the proposed AUD PFS model in terms of the commonly used metrics for PF segmentation. In this evaluation, we have looked at multiple patients with the collected CT scans from varying time periods. The experiment was performed in an external PC with Windows 10 operating system, equipped with Intel Core i9 processor, 32 GB RAM and an NVIDIA GPU with CUDA technology to accelerate deep learning processes. The model is implemented in Python code and takes advantage of Python deep learning frameworks such as TensorFlow and PyTorch to segment the PF. The experimental result of the proposed AUD PFS model is shown in figure 2.

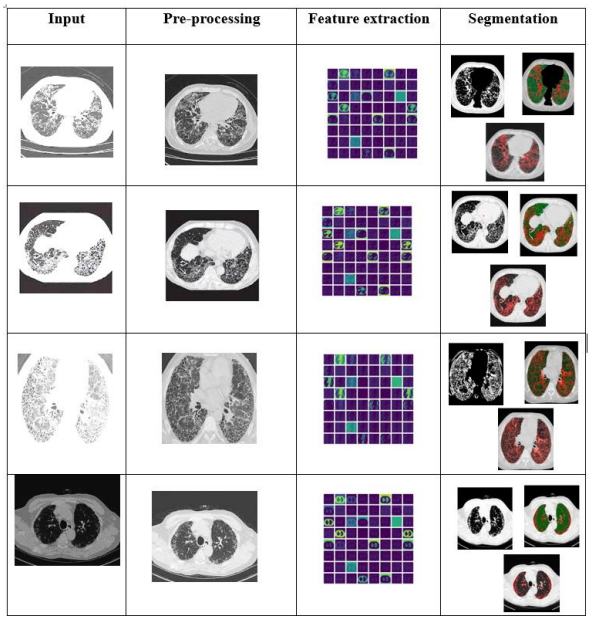

Figure 2: Experimental outcome of the proposed AUD PFS model.

4.1 Performance Analysis

The proposed model's ability to segment pulmonary fibrosis regions is assessed by comparing the anticipated results with the truth. Evaluates correctness and overlaps quality through accuracy (AY), precision (PN), recall (RL), specificity (SY), F1 score (F1-S), Dice Index (DI) and Jaccard Index (JI). The output quality is confirmed by visual examination using binary, color coded and overlay segmentation. The powerful model exhibits high accuracy, clear segmentation boundary and minimum error.

$$AY = \frac{T_P+T_N}{T_P+T_N+F_P+F_N} \quad (9)$$

$$RL = \frac{T_P}{T_P+F_N} \quad (10)$$

$$PN = \frac{T_P}{T_P+F_P} \quad (11)$$

$$SY = \frac{T_N}{T_N+F_P} \quad (12)$$

$$F1-S = 2 * \frac{PN \times RL}{PN+RL} \quad (13)$$

$$DI = \frac{2.T_P}{2.T_P+F_P+F_N} \quad (14)$$

$$JI = \frac{T_P}{T_P+F_P+F_N} \quad (15)$$

From the above equation (9-15) T_P represents True Positive, T_N represents True Negative, F_P represents False Positive, and F_N denotes False Negative in the performance analysis of the PF segmentation of CT image.

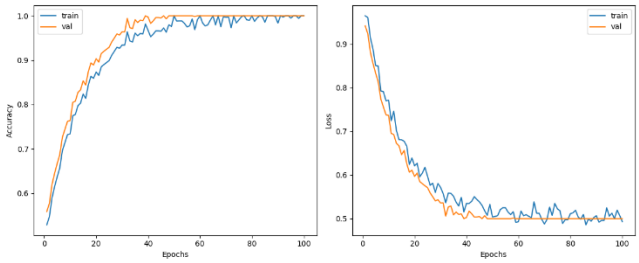

(a) **(b)**

Figure 3: Training and Validation of the proposed AUD PFS model (a) Accuracy Curve (b) Loss curve

The training and validation performance of the proposed AUD PFS model with 100 epochs is shown in Fig. 3. The accuracy graph in figure 3(a) illustrates that the model converged well as training and validation accuracy improve with the initial learning period. The exact correlation between training and validation shows that there is no overfitting and good generalization. As seen in figure 3(b), training and validation loss values have been steadily decreasing with the passage of time, which represents increased learning efficiency. These curves show the durability and stability of the proposed AUD PFS in generating consistent PF segmentation results

4.2 Comparative Analysis

In this section, the proposed AUD PFS model is compared with current models as per specific measures. Existing models were tested for their efficiency and it was determined the AUD PFS model had better accuracy for PF segmentation. The comparative between segmentation networks is illustrated in table 1.

Table 1: Comparison between Segmentation Networks

Network	DI	JI
U Net	0.74	0.76

SegNet	0.80	0.82
Swin UNet	0.88	0.86
Attention UNet	0.97	0.94

Table 2 compares segmentation models utilizing DI and JI which measures the overlap accuracy between predicted and ground truth regions. Attention UNet had the best performance of DI with 0.97 and JI with 0.94, showing superior feature representation and border localization due to long range dependencies. Overall, the findings suggest that the proposed Attention UNet enhance the segmentation accuracy when compared with other Networks.

Table 2: Comparison of different DL Networks with ResNet50

Network	**AY (%)**	**PN (%)**	**SY (%)**	**RL (%)**	**F1-S (%)**
AlexNet	98.24	97.15	96.07	97.17	95.42
ShuffleNet	98.51	97.56	96.21	97.62	96.12
SqueezeNet	98.63	98.07	96.86	98.15	96.85
DenseNet	98.89	98.11	97.64	98.27	97.01
ResNet50 (Ours)	**99.02**	**98.37**	**97.76**	**98.54**	**97.23**

Table 2 compares the effectiveness of various existing networks in extracting PF with the proposed model. AlexNet has lower accuracy of 98.24% because of its restricted feature extraction capability, but ShuffleNet and SqueezeNet increase accuracy by 98.51% and 98.63% through lightweight and efficient learning. DenseNet improves performance by 98.89% allowing for better feature reuse and deeper information flow. The proposed ResNet50 attains the maximum AY of 99.02% and F1-S of 97.23% by merging MobileNet and Efficient Attention, allowing for excellent extraction of both local and global features characteristics for enhanced PF extraction. The proposed AUD PFS model increases the AY by 0.79%, 0.52%, 0.39%, and 0.13% over AlexNet, ShuffleNet, SqueezeNet and DenseNet respectively.

Table 3: Accuracy Comparison of Existing and Proposed AUD PFS model

Authors	**Methods**	**AY (%)**
Dikmen, O., [18]	ResNet18-based U-Net	97.5
Dwivedi et al., [20]	nnU-Net	99.0
Refaee, T., et al., [21]	HCR-DL model	85.3
Maddali, M.V., [22]	CNN	90
Huang, X., [23]	AE-IPF	93.9
Proposed (Ours)	AUD PFS	99.02

Table 3 shows the accuracy comparison of the existing and the proposed AUD PFS model. The comparison of performance shows that the differences in accuracy are mainly due to the ability of each model in representing the complex properties of the lungs. The ResNet18 based U-Net gets a 97.5% accuracy rate thanks to the residual learning, however its shallow depth restricts detailed feature extraction. The nnU-Net achieves 99.0% accuracy thanks to automated architectural optimization and good generalization for medical pictures. The HCR-DL model obtains an accuracy of 85.3%, while the basic CNN reaches 90%, because to a lack of advanced feature learning processes and difficulty with fine-grained fibrosis patterns. The AE-IPF model achieves 93.9% accuracy by enhancing feature representation using latent encoding, however it may lose spatial details. In comparison, the proposed model has the highest AY of 99.02% due to improved feature extraction and greater retention of both spatial and contextual information, resulting in more exact segmentation. The proposed AUD PFS has higher accuracy by 1.53%, 0.02%, 13.85%, 9.11% and 5.17% better than ResNet18-based U-Net, nnU-Net, HCR-DL model, CNN, and AE-IPF respectively.

5. CONCLUSION

This paper presented a novel DL-based AUD PFS for efficient segmentation of Pulmonary Fibrosis disease using CT images. The ResNet50 is used for extraction of the CT images and Attention UNet is used for segmenting the images to Binary segmentation, color-coded segmentation and overlay segmentation of the CT images. The performance of the proposed AUD PFS model was validated using AY, PN, RL, SY, F1-S, DI, and JI. From the experimental result indicate that the proposed AUD PFS model has a high classification AY as 99.02%, F1-Score as 97.23% DI as 0.97 and JI as 0.94 respectively. The proposed AUD PFS model has higher accuracy by 1.53%, 0.02%, 13.85%, 9.11% and 5.17% better than ResNet18-based U-Net, nnU-Net, HCR-DL model, CNN, and AE-IPF respectively. In future, the proposed AUD PFS model focus on improving the model's robustness and generalization by training on larger and more diverse multi-center datasets. The use of advanced architectures, such as vision transformers or hybrid CNN-Transformer models, can improve feature representation and long-term dependency learning. Explainable AI approaches can increase interpretability, making the system more suitable for therapeutic use. Furthermore, refining the model for real-time deployment at a low computing cost and investigating its expansion to multi-class lung disease segmentation can improve its practical relevance in medical diagnostics.

CONFLICTS OF INTEREST

The authors declare that there is no conflict of interest.

FUNDING STATEMENT

Authors did not receive any funding.

ACKNOWLEDGEMENTS

The author would like to express his heartfelt gratitude to the supervisor for his guidance and unwavering support during this research for his guidance and support.

REFERENCES

[1] G. Wang, S. Zhai, G. Lasio, B. Zhang, B. Yi, S. Chen, T.J. Macvittie, D. Metaxas, J. Zhou, and S. Zhang, “Semi-supervised segmentation of radiation-induced pulmonary

fibrosis from lung CT scans with multi-scale guided dense attention," *IEEE Transactions on Medical Imaging*, vol. 41, no. 3, pp. 531–542, 2021. [CrossRef] [Google Scholar] [Publisher Link]

[2] Maetani, N. Tanabe, K. Tanizawa, R. Sakamoto, Y. Shiraishi, Y. Hayashi, M. Uyama, A. Matsunashi, S. Sato, K. Suzuki, and I. Masuda, "Computed tomography morphological assessments of central airways in interstitial lung abnormalities and idiopathic pulmonary fibrosis," *Respiratory Research*, vol. 25, no. 1, p. 404, 2024. [CrossRef] [Google Scholar] [Publisher Link]

[3] S.L. Chantzi, A. Kosvyra, and I. Chouvarda, "Radiomics and artificial intelligence in pulmonary fibrosis," *Journal of Imaging Informatics in Medicine*, vol. 38, no. 5, pp. 2779–2792, 2025. [CrossRef] [Google Scholar] [Publisher Link]

[4] H. Sun, M. Liu, H. Kang, X. Yang, P. Zhang, R. Zhang, H. Dai, and C. Wang, "Quantitative analysis of high-resolution computed tomography features of idiopathic pulmonary fibrosis: a structure-function correlation study," *Quantitative Imaging in Medicine and Surgery*, vol. 12, no. 7, p. 3655, 2022. [CrossRef] [Google Scholar] [Publisher Link]

[5] D. Li, Z. Liu, L. Luo, S. Tian, and J. Zhao, "Prediction of Pulmonary Fibrosis Based on X-Rays by Deep Neural Network," *Journal of Healthcare Engineering*, vol. 2022, no. 1, p. 3845008, 2022. [CrossRef] [Google Scholar] [Publisher Link]

[6] G. Zhang, L. Luo, L. Zhang, and Z. Liu, "Research progress of respiratory disease and idiopathic pulmonary fibrosis based on artificial intelligence," *Diagnostics*, vol. 13, no. 3, p. 357, 2023. [CrossRef] [Google Scholar] [Publisher Link]

[7] Z. Chen, Z. Lin, Z. Lin, Q. Zhang, H. Zhang, H. Li, Q. Chang, J. Sun, and F. Li, "The applications of CT with artificial intelligence in the prognostic model of idiopathic pulmonary fibrosis," *Therapeutic Advances in Respiratory Disease*, vol. 18, p. 17534666241282538, 2024. [CrossRef] [Google Scholar] [Publisher Link]

[8] J. John, A.R. Clark, H. Kumar, A.C. Vandal, K.S. Burrowes, M.L. Wilsher, D.G. Milne, B. Bartholmai, D.L. Levin, R. Karwoski, and M.H. Tawhai, "Pulmonary vessel volume in idiopathic pulmonary fibrosis compared with healthy controls aged > 50 years," *Scientific Reports*, vol. 13, no. 1, p. 4422, 2023. [CrossRef] [Google Scholar] [Publisher Link]

[9] X. Wu, C. Yin, X. Chen, Y. Zhang, Y. Su, J. Shi, D. Weng, X. Jiang, A. Zhang, W. Zhang, and H. Li, "Idiopathic pulmonary fibrosis mortality risk prediction based on artificial intelligence: the CTPF model," *Frontiers in Pharmacology*, vol. 13, p. 878764, 2022. [CrossRef] [Google Scholar] [Publisher Link]

[10] W.K. Cheung, A. Pakzad, N. Mogulkoc, S. Needleman, B. Rangelov, E. Gudmundsson, A. Zhao, M. Abbas, D. McLaverty, D. Asimakopoulos, and R. Chapman, "Automated airway quantification associates with mortality in idiopathic pulmonary fibrosis," *European Radiology*, vol. 33, no. 11, pp. 8228–8238, 2023. [CrossRef] [Google Scholar] [Publisher Link]

[11] E. Vincenzi, A. Fantazzini, C. Basso, A. Barla, F. Odone, L. Leo, L. Mecozzi, M. Mambrini, E. Ferrini, N. Sverzellati, and F.F. Stellari, "A fully automated deep learning pipeline for micro-CT-imaging-based densitometry of lung fibrosis murine models," *Respiratory Research*, vol. 23, no. 1, p. 308, 2022. [CrossRef] [Google Scholar] [Publisher Link]

[12] Y. Chen, H. He, L. Luo, K. Liu, M. Jiang, S. Li, X. Zhang, X. Yang, and Q. Liu, "Studying pulmonary fibrosis due to microbial infection via automated microscopic image analysis," *Frontiers in Microbiology*, vol. 14, p. 1176339, 2023. [CrossRef] [Google Scholar] [Publisher Link]

[13] A.H. Syed, T. Khan, and S.A. Khan, "Deep transfer learning techniques-based automated classification and detection of pulmonary fibrosis from chest CT images," *Processes*, vol. 11, no. 2, p. 443, 2023. [CrossRef] [Google Scholar] [Publisher Link]

[14] J.R.F. Raj, K. Vijayalakshmi, S.K. Priya, and A. Appathurai, "Brain tumor segmentation based on kernel fuzzy c-means and penguin search optimization algorithm," *Signal, Image and Video Processing*, vol. 18, no. 2, pp. 1793–1802, 2024. [CrossRef] [Google Scholar] [Publisher Link]

[15] J.L. Wang, X.R. Cheng, Z.Y. Meng, and Y.L. Wang, "Impact of total cerebral small vessel disease score on ophthalmic artery morphologies and hemodynamics," *Journal of Translational Medicine*, vol. 21, no. 1, p. 65, 2023. [CrossRef] [Google Scholar] [Publisher Link]

[16] S. Kaur, S. Gupta, D. Gupta, S. Juneja, A. Nauman, M. Khan, I. Husain, A. Islam, and S. Mallik, "High-accuracy lung disease classification via logistic regression and advanced feature extraction techniques," *Egyptian Informatics Journal*, vol. 29, p. 100596, 2025. [CrossRef] [Google Scholar] [Publisher Link]

[17] T. Sanida, M.V. Sanida, A. Sideris, and M. Dasygenis, "Optimizing Lung Condition Categorization through a Deep Learning Approach to Chest X-ray Image Analysis," *BioMedInformatics*, vol. 4, no. 3, pp. 2002–2021, 2024. [CrossRef] [Google Scholar] [Publisher Link]

[18] O. Dikmen, "Deep Learning Models for the Detection and Classification of COVID-19 and Associated Lung Diseases Using X-Ray Images," *Artificial Intelligence Theory and Applications*, vol. 4, no. 2, pp. 121–142, 2024. [CrossRef] [Google Scholar] [Publisher Link]

[19] M. Thillai, J.M. Oldham, A. Ruggiero, F. Kanavati, T. McLellan, G. Saini, S.R. Johnson, F.X. Ble, A. Azim, K. Ostridge, and A. Platt, "Deep learning–based segmentation of computed tomography scans predicts disease progression and mortality in idiopathic pulmonary fibrosis," *American Journal of Respiratory and Critical Care Medicine*, vol. 210, no. 4, pp. 465–472, 2024. [CrossRef] [Google Scholar] [Publisher Link]

[20] K. Dwivedi, M. Sharkey, S. Alabed, C.P. Langlotz, A.J. Swift, and C. Bluethgen, "External validation, radiological evaluation, and development of deep learning automatic lung segmentation in contrast-enhanced chest CT," *European Radiology*, vol. 34, no. 4, pp. 2727–2737, 2024. [CrossRef] [Google Scholar] [Publisher Link]

[21] T. Refaee, Z. Salahuddin, A.N. Frix, C. Yan, G. Wu, H.C. Woodruff, H. Gietema, P. Meunier, R. Louis, J. Guiot, and P. Lambin, "Diagnosis of idiopathic pulmonary fibrosis in high-resolution computed tomography scans using a combination of handcrafted radiomics and deep learning," *Frontiers in Medicine*, vol. 9, p. 915243, 2022. [CrossRef] [Google Scholar] [Publisher Link]

[22] M.V. Maddali, A. Kalra, M. Muelly, and J.J. Reicher, "Development and validation of a CT-based deep learning algorithm to augment non-invasive diagnosis of idiopathic pulmonary fibrosis," *Respiratory Medicine*, vol. 219, p. 107428, 2023. [CrossRef] [Google Scholar] [Publisher Link]

[23] X. Huang, W. Si, X. Ye, Y. Zhao, H. Gu, M. Zhang, S. Wu, Y. Shi, X. Gui, Y. Xiao, and M. Cao, "Novel 3D-based deep learning for classification of acute exacerbation of idiopathic pulmonary fibrosis using high-resolution CT," *BMJ Open Respiratory Research*, vol. 11, no. 1, 2024. [CrossRef] [Google Scholar] [Publisher Link]

AUTHORS

L. Godlin Atlas is an accomplished academician with over 15 years of teaching experience across various institutions. He is currently serving as an Associate Professor in the Department of Computer Science and Engineering at Bharath Institute of Science and Technology, Chennai. He earned his Ph.D. in Computer Science and Engineering from Manonmaniam Sundaranar University, Thirunelveli, in 2018. He completed his Bachelor of Technology in Information Technology from CSI Institute of Technology and his Master of Engineering from The Indian Engineering College, Nagercoil. Dr. L.Godlin Atlas has made significant contributions to research, having authored more than 25 papers published in reputed national and international journals and conferences. His work has been indexed in prominent databases such as SCI, Scopus, Web of Science, and Google Scholar. He is an active member of several professional organizations, including IET, ISTE, IAENG, and IACSIT. His research interests encompass Medical Image Processing, Networking, Artificial Intelligence, and Machine Learning.

V. Vaishnavi is received her B.E degree in Electrical and Electronics Engineering from Sethu Institute of Technology, virudhunagar, Tamilnadu, India and her M.E degree in Applied Electronics in Anna University of Technology,Tirunelveli, Tamilnadu, India. She has teaching experience of about 10 yrs. Initially she worked as an Assistant Professor in Narasu's sarathy institute of Technology, Salem.& Vickram College of Engineering,Sivagangai.. At present, she is working as an Assistant Professor in "Sethu Institute of Technology, Virudhunagar, Tamilnadu, India". She has published more than 4 papers in National InternationalConferences and also 1 paper in reputed journal. And Her areas of interest include Signal Processing, and communication.

Arrived: 25. 01. 2026
Accepted: 23. 02. 2026